J Mater Sci (2007) 42:7872–7881
DOI 10.1007/s10853-007-1660-4

Experimental evaluation of the double torsion analysis on soda-lime glass

M. A. Madjoubi · M. Hamidouche · N. Bouaouadja · J. Chevalier · G. Fantozzi

Received: 28 October 2006 / Accepted: 5 March 2007 / Published online: 30 May 2007
© Springer Science+Business Media, LLC 2007

Abstract According to the classical model developed by Evans and co-workers on the double torsion test [(1972) J Mater Sci 7:1137 and (1973) J Testing Eval 1:264], the stress intensity factor is independent of the crack length. Recent applications and analysis question this independency (Chevalier et al (1996) Cer Inter 22:171, Ciccotti et al (2000) Inter J Rock Mech Min Sci 37:1103). This work consists of using samples with different lengths of a typical brittle material (a soda-lime glass) in order to discuss on the validity of the different equations proposed to analyse the DT technique. Experimental compliance tests always showed linear variations with crack length. Successive relaxation tests revealed, however, a clear dependency of the stress intensity factor on crack length. This dependency, observed through the non reproducibility of the V–K_I diagrams, is reduced as the sample length increases. The corrections proposed by Chevalier and Ciccotti on Evans model revealed that their applications remain limited to the sample and the loading configurations used by the authors. The application of Evans model without correction is conditioned by the use of sufficiently long samples and advanced crack lengths.

M. A. Madjoubi (✉) · M. Hamidouche · N. Bouaouadja
Laboratoire des Matériaux Non Métalliques, Dpt. OMP, Faculté des Sciences de l'Ingénieur, Université Farhat Abbas, 19000 Sétif, Algérie
e-mail: medmadjoubi@yahoo.com

J. Chevalier · G. Fantozzi
Laboratoire GEMPPM, Bat Blaise PASCAL, INSA, 20 Avenue Albert Einstein, Villeurbanne 69621, France

Introduction

To evaluate directly Crack Growth versus Stress Intensity Factor (V–K_I)diagrams on brittle materials, it is recommended to use techniques allowing stable crack propagation. Examples of such methods are the double cantilever beam (DCB), loaded by a constant moment or by compression [1, 2], the double cleavage drilled compression method (DCDC) [3] and the double torsion test (DT). The DT method, initially introduced by Outwater and Gerry [4], was mainly developed by Evans and Williams [5, 6]. It is characterized by simple sample geometry and a 4 points bending type loading configuration (Fig. 1a). This configuration leads to a faster propagation on the tensile side than that on the compressive side, generating a curved crack front (Fig.1b).

Evans [5] showed that the V–K_I diagram could be directly evaluated on a single sample using a constant displacement loading (relaxation method). This test consists in recording the load–time relationship, without having to follow the evolution of the crack. The non necessity to measure the crack length constitutes the major advantage of this technique, permitting its use on opaque materials, in hostile environments and at high temperatures.

The developed analysis [5, 6] is essentially based on the following hypotheses

- The sample is considered constituted of two bars loaded in simple torsion. The effect of the compression or shearing stresses, generated by the contact between the two bars, is disregarded.
- The deformation of the non-cracked part of the sample is supposed negligible in comparison to the one of the cracked part.

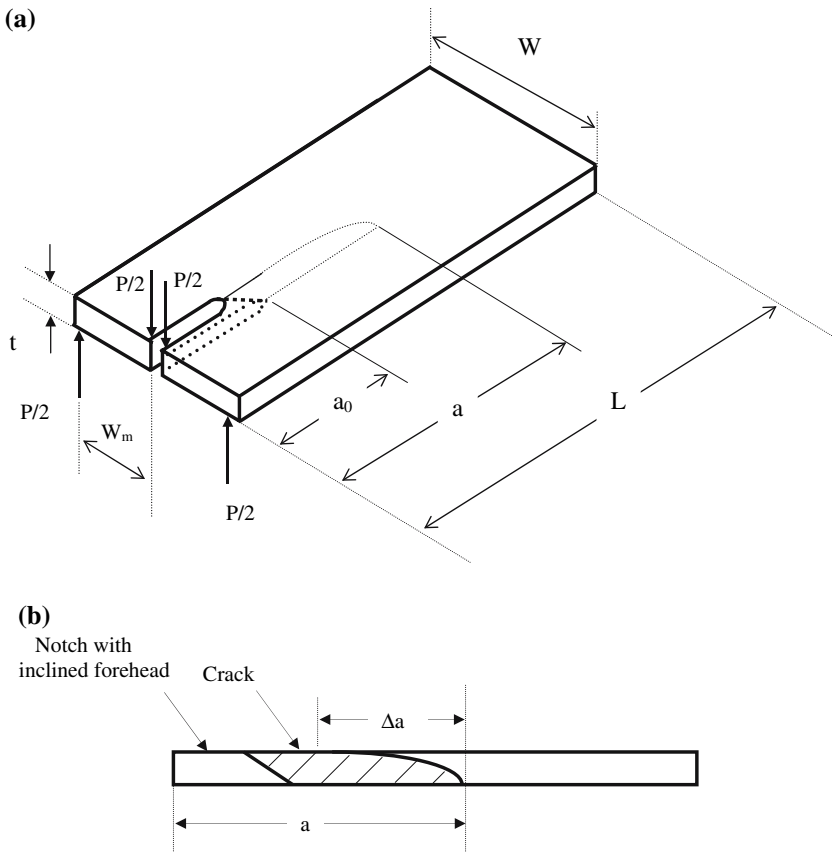

Fig. 1 Geometric characteristics (**a**) and curved crack front (**b**) of double torsion specimen

- The crack front is straight and independent of the crack length.
- The fracture mode is the ''I'' opening type.

Using the first two hypotheses, Williams and Evans [6] showed that the DT sample compliance varies linearly as a function of the crack length, according to the following relation:

$$C = B \cdot a \tag{1}$$

with B, a constant dependent on the sample dimensions (W, t), the loading configuration (W_m) and the shear modulus μ, defined as

$$B = \frac{3W_m^2}{Wt^3\mu\psi(T)} \tag{2}$$

The factor $\psi(T)$ was introduced, later by Fuller Jr [7], to take into account the effect of the sample thickness. It is defined by the following expression:

$$\psi(T) = 1 - 0.6302T + 1.2Te^{-\pi/T} \tag{3}$$

where T corresponds to $(2t/W)$. The definition of this factor was derived from the analysis of the DT compliance based on the theory of the torsion of rectangular bars developed by Timoshenko [8].

Experimental tests conducted on different materials [5, 6, 7] confirm the linear variation of compliance written in the general form:

$$C = B \cdot a + D \tag{4}$$

The value of the ordinate at the origin D, although small, remains quantifiable.

The sample compliance is related to the strain-energy-release rate for crack extension G by the expression:

$$G = \frac{P^2}{2}\left(\frac{dC}{dA}\right) \tag{5}$$

where A is the crack surface. By supposing that the crack front profile remains constant, the Eq. (5) becomes:

$$G = \frac{P^2}{2t}\left(\frac{dC}{da}\right) \tag{6}$$

With regard to Eqs. (1) and (2), the expression of G is:

$$G = \frac{P^2}{2t}B = \frac{3P^2W_m^2}{2Wt^4\mu} \tag{7}$$

Using the relationship between the stress intensity factor K and the strain-energy-release rate for crack extension G

in mode I, the expression of stress intensity factor K_I that ensues from this analysis is:

$$K_I = H \cdot P \tag{8}$$

where H, depending on the assumption of plane strain or a plane stress state, is defined by:

$$H = \sqrt{\frac{\mu B}{(1 \mp \nu)^{\pm 1} t}} \tag{9}$$

where ν is the material Poisson coefficient. The superior and lower signs are assigned respectively to the plane strain and stress states. For brittle materials, plane strain state is considered.

Evans [5] showed that the failure of brittle materials is exclusively of the mode I type by comparing, on a soda-lime glass, the measured critical strain-energy release rate G_c obtained with double torsion with the mode I G_{Ic} obtained by other methods. The expression of the crack propagation velocity for the relaxation tests (loading at constant displacement) is:

$$V = -\phi \frac{P_{i,f}}{P^2} \left(a_{i,f} + \frac{D}{B} \right) \frac{dP}{dt} \tag{10}$$

where $P_{i,f}$ and $a_{i,f}$ are respectively the applied load and the crack length corresponding to the initial or final state. The factor ϕ was introduced to correct the effect of the curvature of the crack front on the crack velocity. Assimilating the crack front profile to an inclined straight line, Evans [5] defined the factor ϕ by the relation:

$$\phi = t / \sqrt{\Delta a^2 + t^2} \tag{11}$$

On the basis of the real curvature of crack front, Pollet and Burns [9] defined this factor by the expression:

$$\phi = \left[(1/t) \int_0^t \sin \theta^{1/n} dy \right]^n \tag{12}$$

θ is the variable angle that the tangent makes in every point of the crack front with the horizontal direction and n, the sub-critical crack growth exponent of the law ($V = AK^n_I$). The integral is made along the sample thickness. If the crack front is assimilated to a straight line, the expression (12) reduces to Eq. (11). On samples with weak thickness of glass and alumina, Evans found experimentally that this factor corresponds to about 0.2. The nominal velocities (corresponding to those of the crack front tip) determined by double torsion, are 5 times more important than those determined by the DCB method, where the crack front is straight [5].

In the same context, another analysis, made by Shetty et al. [10], shows how to determine the average velocity and its direction on the basis of the real crack front in relation to the nominal velocity.

From the different experimental works achieved on the use of the double torsion test, it appears that the validity of Evans model is conditioned by some recommendations. It is, first of all, advised to use long samples ($L/W > 2$) with weak thicknesses [11, 12]. Moreover, the initial crack must be propagated far enough to admit that the non-cracked part is not deformed in comparison to the cracked part. The crack length work domain must, in general, be located far from the extremities of the sample, because the compliance variation is established to be non linear when approaching them. Different researchers proposed a work domain where K_I can be considered independent of the crack length [12–14]. As an example, Trantina [13] suggested on the basis of a bi-dimensional finite element analysis, a work domain, applicable on samples with dimensions such as their ratios are (t:W:L = 1:10:20). This domain is defined by ($0.55W < a < L - 0.65W$).

Until relatively recent works achieved by Chevalier et al. [15] and by Ciccotti et al. [16–18], the scattering of the results or the shift of the V–K_I curves observed on some ceramics were usually explained by the influence of the microstructure [11, 12]. The use of Evans model (Eq. 8) by Chevalier et al. on a stabilized zirconia (3Y-TZP) characterized by very fine grains and a strengthening zone not exceeding about ten microns, revealed a systematic shift of the V–K_I curves toward lower K_I values as the length of the initial crack increases. The DT tests were made on samples with ratios (t:W:L = 1:10:20) within the so called linear region. The authors proposed, through an experimental analysis on this material, to introduce a correction factor that takes into account the effect of the crack length. The expression of the corrected empirical equation is:

$$K_I = HP(a/a_0)^{\alpha} \tag{13}$$

where α corresponds to about 0.2 and a_o is the notch length. The crack length, for a constant displacement loading, is defined by the relation:

$$a = P_{i,f}(Ba_{i,f} + D)/B - D/B \tag{14}$$

The authors showed that the dependence of K_I on crack length is caused by the effect of the non fractured ligament observed on the compressive side of the samples.

Through a comprehensive finite element analysis (FEA), Ciccotti et al. [16, 17] showed that Evans model describes the DT sample compliance only on a limited area around the centre. This three-dimensional FEA analysis is more realistic than the one presented by Trantina [13]. Noticing

the non linearity of compliance on a large crack lengths domain, the authors proposed to introduce corrective factors in function of the crack length $\xi(a)$ and $\Psi(a)$, on respectively the compliance C and its derivative dC/da, in order to correct Evans model. The published corrective factors concern four particular samples geometries with different L/W ratio. They were derived from this analysis, for five different crack length values, covering a large interval. The variation curves of these coefficients with crack length can be obtained by non linear fitting on the basis of the five recorded values.

The corrected expressions of C, K_I and V are respectively:

$$C(a) = \xi(a)Ba \tag{15}$$

$$K_I(a,P) = \sqrt{\psi(a)}\mathrm{HP} \tag{16}$$

$$V = -\phi \frac{\xi(a_{i,f})}{\psi(a)} \frac{a_{i,f}P_{i,f}}{P^2} \frac{dP}{dt} \tag{17}$$

It is important to underline that the direct use of the recorded values is conditioned by the type of dimensions ratios (t:W:L) of the samples used by the authors. In the case where the sample geometry is different, it is possible to do linear interpolations between the values of the different geometries proposed. Examples of applications were published in this sense by the authors [18].

The results of this analysis reveal that, without the use of the correction factors proposed, an under-estimation of the sub-critical crack growth exponent n up to 30% can occur. This should happen even though one takes care to work far from the sample extremities. With the introduction of these factors, on the contrary, an improvement of the results is possible within a larger work domain.

The purpose of our work is to examine experimentally the dependence of the compliance and the stress intensity factor in relation to the crack length in order to evaluate the different equations proposed of the DT test. Compliance and successive relaxations tests were conducted on soda-lime glass samples of variable length.

Soda-lime glass was chosen as a model material because of its typical brittleness associated with homogeneity, isotropy and transparency. This last characteristic allows observing the crack front evolution during the propagation. It is also a material whose sub-critical crack growth characteristics were extensively studied by different methods [19–22].

Experimental procedure

The glass samples used for the compliance and relaxation tests were rectangular plates of thickness (t = 3mm), of width (W = 40 mm) and of variable lengths (L = 60, 80, 100 and 120 mm). They were cut from the same glass sheet and were notched in the middle of the loading edge on a length varying from 8 mm to 15 mm with a diamond-covered disk of 0.3 mm thickness. The samples underwent an annealing treatment after the different machining operations in order to eliminate the residual stresses. All test samples were prepared without guiding groove. This simplification permits to eliminate the effect of stress concentrations these grooves generate [23]. A geometrical description of the sample type with its particularities (inclined forehead notch, curved pre-crack front and without guiding groove) is presented on Fig. 1.

It can be noticed that the notch presents an inclined forehead whose long part is on the tensile side. The notch inclination facilitates the propagation of the pre-crack, always evolving more quickly on the tensile side than on the compressive side with a curved crack front (Fig. 1b). Δa represents the crack propagation difference between the two sides. The 4 points bending loading configuration leading to the torsion of the two sample parts, is assured by a cylindrical roller placed in contact with the two sides of the notch and two lower supporting rollers (Fig. 2). The load, so applied, is transmitted in a symmetrical manner. The rear rollers serve only to position the sample in a symmetrical manner before applying the load.

The orientation of the crack propagation in the middle of the plate is facilitated by the application of a Vickers indentation at the tensile side notch end with a load of 10 N. This indentation must be oriented so that the radial cracks are perpendicular to the sides of the sample (Fig. 3a). It is applied after the annealing treatment because it was noticed that the residual stresses, induced by this indentation, help to reduce the necessary critical load for initiating the pre-crack and consequently increase its stability. On Fig. 3b, the photograph shows that the crack starts at the level of the indentation placed at the notch end and follows the orientation of the longitudinal radial crack. The longitudinal orientation of the pre-crack can be assured without a guiding groove with the help of this indentation

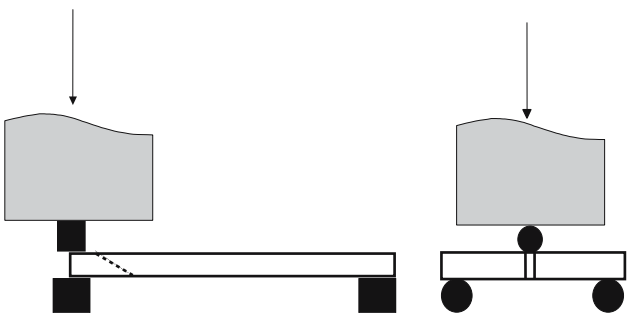

Fig. 2 Loading configuration used for double torsion tests

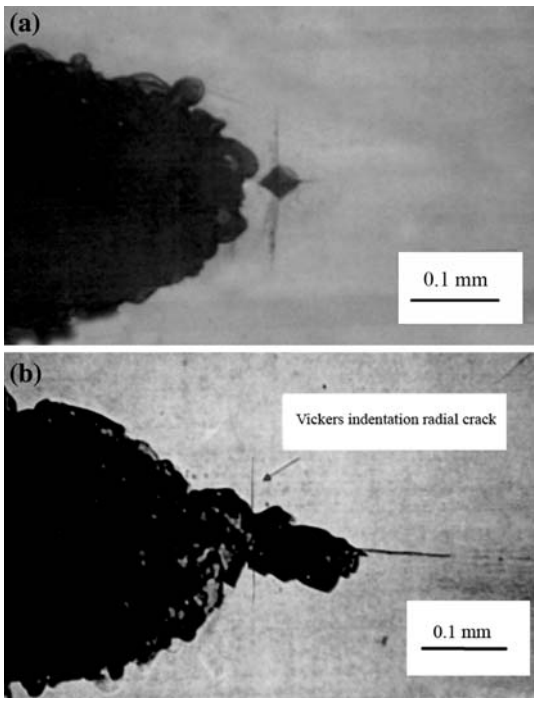

Fig. 3 Photographs showing the Vickers indentation location at the notch end (**a**) and the initiation of a pre-crack from indentation (**b**)

associated to a good alignment of the sample in the loading device [24].

The pre-cracking operation is carried out with a very low loading velocity (0.01 mm/min) on a universal electro-mechanical testing machine (Schenck). The detection of the critical load initiating the pre-crack is revealed by observation of the variation of the applied load as a function of the displacement on a recording chart. The critical load is characterized by the beginning of the non linearity of the load–displacement curve due to the fast drop of the applied load provoked by the initiation of the crack. The unloading of the sample must be done quickly when the critical load is reached in order to limit the pre-crack propagation.

All compliance and relaxation tests were achieved in the laboratory ambient air conditions. The compliance was determined for different crack lengths on each sample by recording the loading point displacement variation during cyclic loadings. A minimum of three loading–unloading cycles for every crack length were recorded at a relatively high speed (0.3 mm/min). The applied loads were kept less than 20 N in order to avoid crack propagation. The displacement was measured using a sensor placed in contact of the sample at the notch extremity. The compliance is evaluated from the slopes of the recorded lines ($C = \Delta y/\Delta P$).

In order to test the compliance evolution close to the extremities, some complementary tests were made on samples continuously notched on different lengths without pre-cracking. This procedure was necessary because it was not easy to obtain very short natural cracks or to test the compliance of samples with very long natural cracks. The propagation becomes unstable when the crack approaches the extreme edge.

The relaxation test consists in loading a sample with a fast enough speed ($V = 0.5$ mm/min) until an initial load value P_i close to the critical load P_c leading the pre-crack and to stop the displacement of the machine crosshead. A relaxation of the applied load occurs as the crack evolves by the effect of the surrounding humidity. The recording of the load relaxation with time on a chart permits to evaluate the sub-critical propagation velocity in relation to the applied stress intensity factor according to Eqs. (8) and (10). The loads applied for the different relaxation tests did not exceed 50 N. With such loads, the testing machine (Schenck, maximum loading capability 5 kN), characterized by high elements rigidity (Stiffness higher than 10 kN/mm), did not cause any appreciable secondary relaxation.

The determination of the velocity requires to know the initial or final load $P_{i,f}$ and the initial or final corresponding crack length $a_{i,f}$ (Eq. 10). It is preferable to use the final load and the corresponding final length that can be measured with accuracy at the end of the relaxation test without influence of the environment. The initial crack length value can be subject to a certain imprecision because it can evolve during loading under the effect of the environment before the relaxation starts. This happens particularly when the initial applied load is close to the critical load.

The evaluation of the stress intensity factor (Eq. 8) requires the determination of the constant H that depends on the sample dimensions and Poisson coefficient. Being independent of the sample length, the constant H does not vary with the different samples geometries used in this study.

The relaxation test duration is limited to a half hour. Beyond this period, the variations of the ambient temperature can have an influence on the recorded load relaxation. This type of test enables to determine with reliability sub-critical crack velocities between 10^{-3} m/s and 10^{-7} m/s. Within such an interval, we can clearly distinguish the three sub-critical crack growth domains. Without a control of the test environment conditions, reaching lower velocities requires to work at constant loading and to follow the crack evolution [24].

Results

Compliance tests

The results of the compliance variation versus crack length on three samples of dimensions ($3 \times 40 \times 80$mm) are presented in Fig. 4. We associated to these experimental results, for a comparison, the theoretical compliance

variations defined by Evans (Eq. 2) and by Ciccotti (Eq. 15) with the introduction of the corrective coefficients $\xi(a)$.

The experimental results show a linear compliance variation whose slope ($3.12 \times 10^{-5}\mathrm{N}^{-1}$) is comparable to the one defined theoretically by Evans ($3 \times 10^{-5}\mathrm{N}^{-1}$). There is no obvious non linearity of the compliance for low crack length values near the loading edge. The extreme compliance values were omitted because continuously notched samples led in general to lower values than those obtained with the natural crack growth.

The simulated compliance variation curve is based on the use of the correction coefficients $\xi(a)$ corresponding to a sample geometry ($3 \times 40 \times 70$mm) close to one of the cases considered by Ciccotti et al. [17]. This curve shows a weak non linearity, which could be hardly detected experimentally. In both theoretical curves (Evans and Ciccotti), the ordinate at the origin is null ($D = 0$).

On Fig. 5, are represented the results of compliance variation for four samples with different lengths (L = 60, 80, 100 and 120 mm). These results show that the variations are in each case practically linear. The different slopes ($B = (2.86 \pm 0.32) \times 10^{-5}$) are comparable to the one defined theoretically by Evans. A small variability of the ordinate at the origin is noticed with the variation of the samples length (($D = 3.305 \pm 0.32) \times 10^{-7}$). So far, these results do not reveal a clear interrelationship between D coefficient and the sample length.

Successive relaxation tests

An example of V–K_I diagrams, obtained from four successive relaxations (designated by R1, R2, R3 and R4) on a same sample with dimensions ($3 \times 40 \times 80$mm), is shown on Fig. 6.

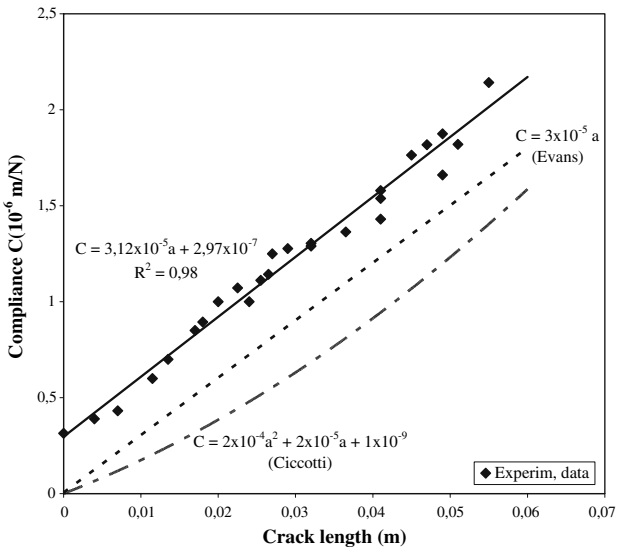

Fig. 4 Experimental and theoretical (Evans, Ciccotti) compliance variation with crack length

For these tests, relatively weak initial loads ($P_\mathrm{i} \approx 30$ N) were used in order to work on the first domain (stage I) of the V–K_I diagram. An evident dependence of the stress intensity factor, calculated from Evans expression (Eq. 8), with crack length can be noticed from this figure. With the increase of the initial crack length, it appears a shift, nearly parallel, of the curves toward greater velocities and lower stress intensity factors. The sub-critical crack growth exponent n varies between 16 and 19 and $\log(A)$ varies between –0.2 and –2. The systematic curve shift as the initial crack length increases, which can not be attributed to the structure or any changing process of the material (soda-lime glass), is inevitably due to the use of Evans expression of K_I (Eq. 8).

The results of other successive relaxation tests, made on samples having different lengths (L/W = 1.5, 2, 2.5 and 3) with the use of larger initial loads (40N < P_i < 50N), are shown in Fig. 7.

It can be noticed that the K_I dependence on crack length decreases as the L/W ratio increases. The obtained results of three successive relaxations for the longest sample, when L/W = 3, show an acceptable reproducibility of the diagrams, except for few values corresponding to the shortest crack lengths (some values of the first relaxation). It seems that the domain where the stress intensity factor is independent on the crack length becomes more important when the length of the sample increases. The initial crack must also be long enough to avoid the loading edge and notch effect.

For the shortest sample (L/W = 1.5), a crack growth instability, leading to its breakage, was noticed early in the second relaxation as the crack approaches the ending edge. For nearly the same initial loading and crack lengths conditions, the crack growth instability problem is avoided as the sample length increases.

Application of corrected equations proposed by Chevalier and Ciccotti

The application of the corrected equation presented by Chevalier (Eq. 13), on the previous examples, succeeded to reunify the diagrams in the case where L/W corresponds to 2 (samples with dimensions $3 \times 40 \times 80$ mm). This case is presented on Fig. 8 (case 8b). The reunification of the diagrams for the other cases was possible with a change of the exponent α value (Fig. 8 a, c and d). As the ratio L/W decreases from 3 to 1.5, the exponent increases from 0 up to 0.22. For the longest sample (L/W = 3), no amelioration was noticed with the corrected equation ($\alpha \approx 0$). Exponent values greater than 0.01 brought more dispersion on the diagrams in this case.

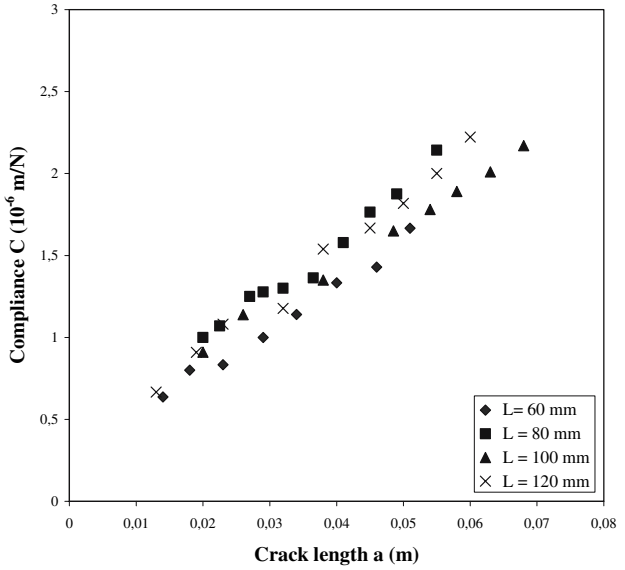

Fig. 5 Compliance variation with crack length for samples of different lengths

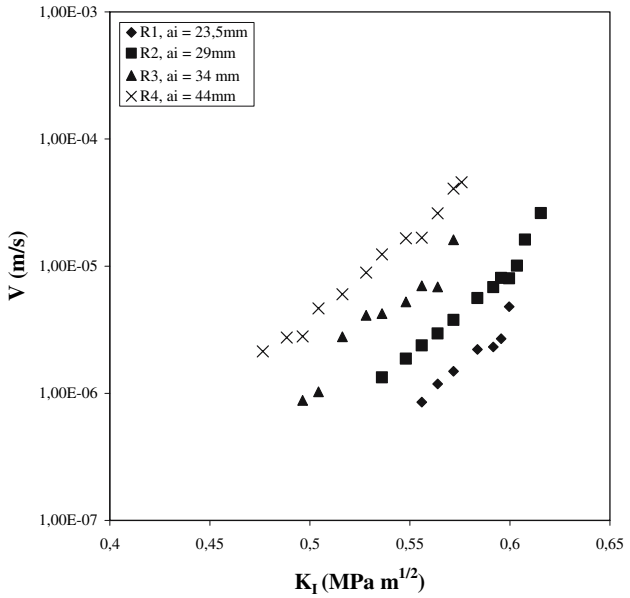

Fig. 6 V–K_I diagrams obtained by 4 successive relaxations on a sample with dimensions 3 × 40 × 80mm

The diagrams reunification for the other cases occurs with a shift toward greater K_I values. This shift increases with the exponent α value. In general, it was noticed that the sub-critical crack growth exponent n values of the first domain (I) on the corrected diagrams ($20 < n < 30$) are slightly greater than the admitted values for soda-lime glass ($16 < n < 20$).

The application of the corrections proposed by Ciccotti (Eqs. 16 and 17) was made on a sample with dimensions (3 × 40 × 70mm) and a notch length of 8 mm. The

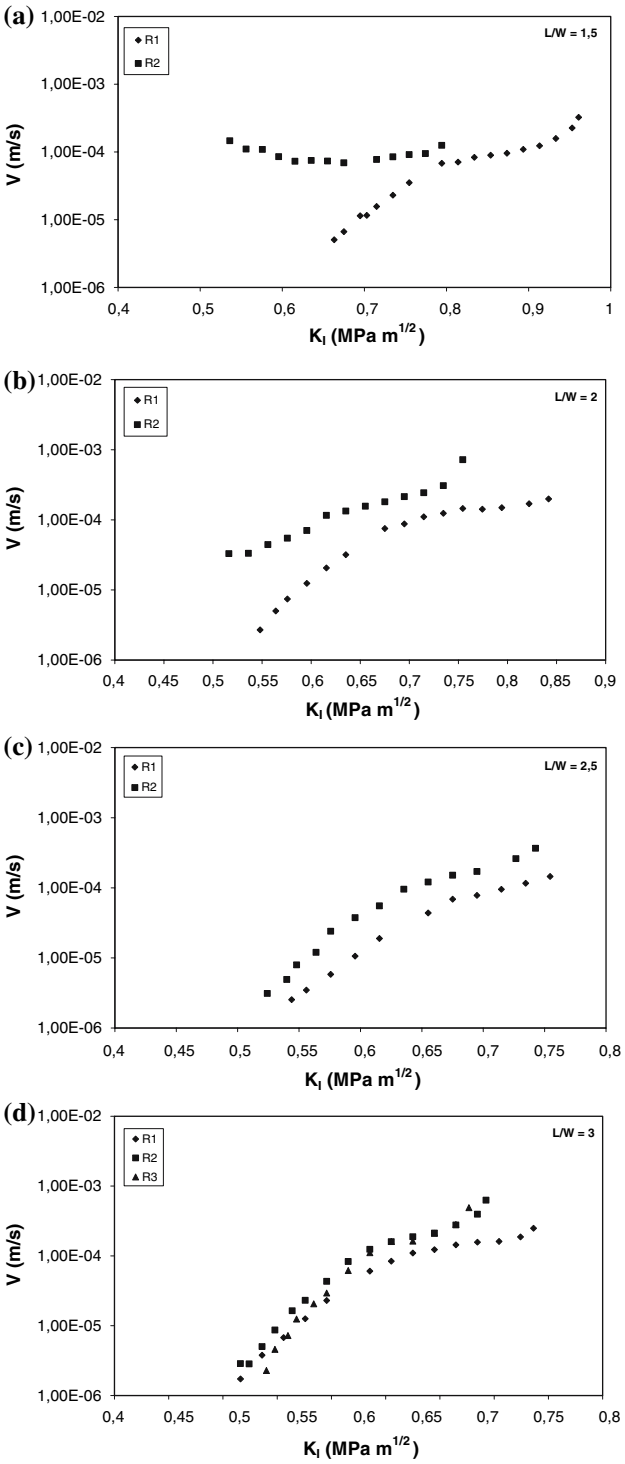

Fig. 7 V–K_I diagrams obtained by successive relaxations on samples with different lengths: (**a**) 3 × 40 × 60mm (L/W = 1.5) (**b**) 3 × 40 × 80mm (L/W = 2) (**c**) 3 × 40 × 100mm (L/W = 2.5) (**d**) 3 × 40 × 120mm (L/W = 3)

variations of the corrective factors $\xi(a)$ and $\Psi(a)$ used for this example are presented on Fig. 9. These variations are based on the corrective factors corresponding to a closer

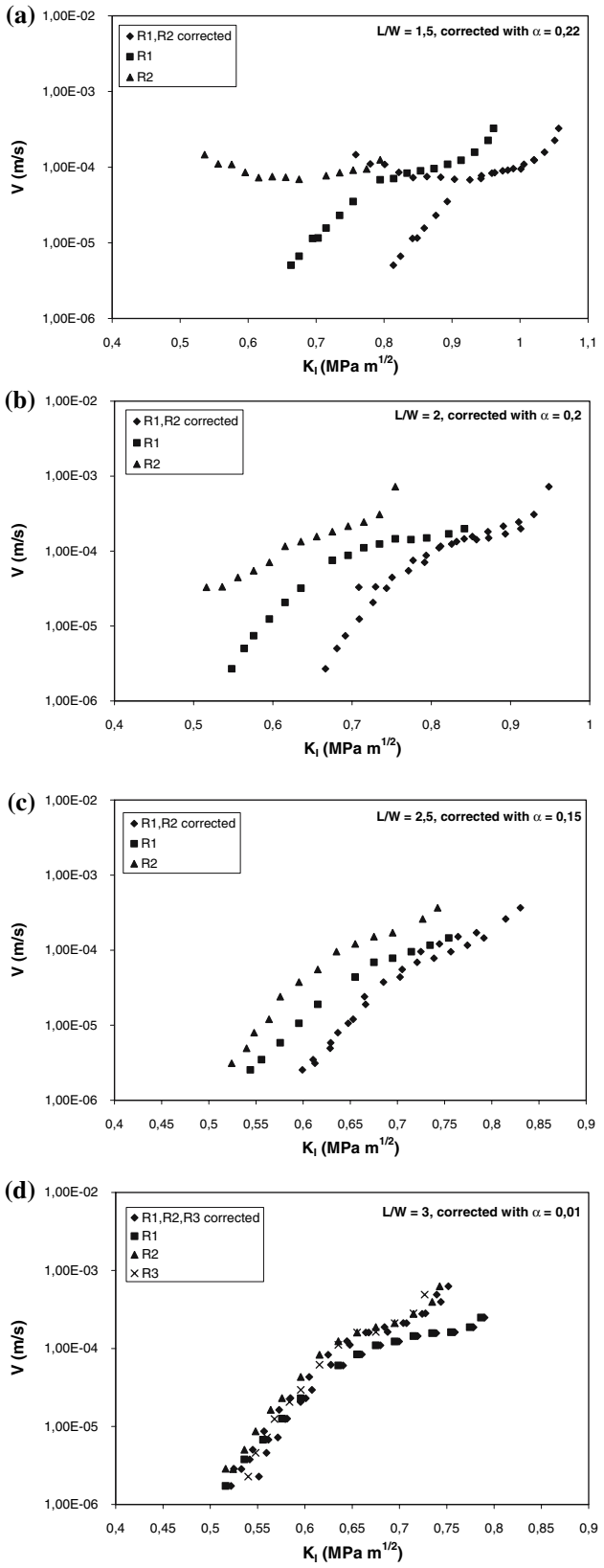

Fig. 8 Application of the correction proposed by Chevalier et al. on the successive relaxations of the samples with different L/W ratio (notice the dependence of the exponent α on L/W)

case studied by the author [16, 17], using the necessary scaling ratio on crack lengths. Because of the notch presence, the first value of each factor, in Ciccotti's work, was not derived from the simulation as the rest of the values, but estimated from the results obtained on unnotched samples [17].

Four successive relaxations were made on this sample using an initial load ($P_i \approx 30$ N). The corrections obtained through the use of Eqs. 16 and 17 on these relaxations are shown in Fig. 10.

The first remark to be made is the distinction of the results obtained on the first relaxation (Fig. 10a). The applied corrective factors on the shortest crack lengths led to an abnormal increase of the stress intensity factor K_I values as crack grows. The correction on the remaining relaxations regroups the values well enough into one straight line. This line is located at the level of the fourth relaxation values with a sub-critical crack growth exponent n equal to 18.3.

It was noticed through data checking that the distinction of the first relaxation was related to the effect of the low given value (0.52) of the estimated $\psi(a)$ factor. This is probably due to the difference in the loading configurations used (use of rollers as supports instead of balls and position of the applied load relative to the edge). The increase of

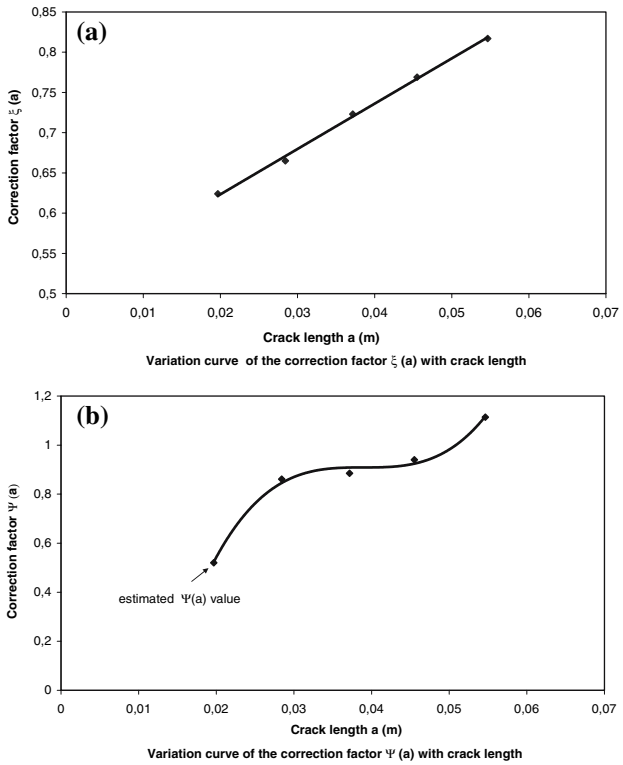

Fig. 9 Variations of the correction factors $\xi(a)$ and $\Psi(a)$ proposed by Ciccotti et al. for a sample with dimensions (3 × 40 × 70mm)

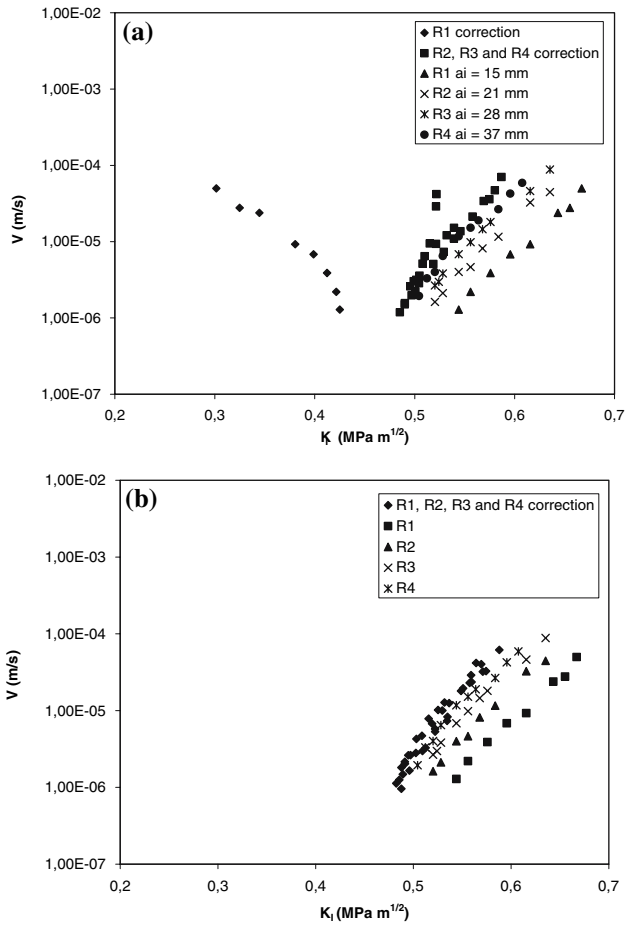

Fig. 10 Application of the correction factors $\xi(a)$ and $\Psi(a)$ on 4 successive relaxations (sample of dimensions 3 × 40 × 70mm). With the given estimated $\Psi(a)$ factor 0.52 (**a**) and with the modified $\Psi(a)$ value 0.8 (**b**)

this estimated value up to 0.8 led to a close reunification of all four relaxations on the same line (Fig. 10b).

For comparison, the preceding example was also corrected according to Chevalier's corrected equation whose results are presented on Fig. 11. The equation α coefficient that reunites best the 4 diagrams, in this case, corresponds to 0.16. The comparison of this value with the previous ones shows that the exponent dependence in relation to the sample geometry (sample and notch length) remains to be established. As for the previous cases (Fig. 8), the diagrams reunification occurs at greater K_I values. The sub-critical crack growth exponent n obtained was 20.5.

Crack front observations

The post-mortem observations of the fractured samples showed no appreciable variation of the crack front profile in relation to the crack length. A photograph example of the crack front profile with a descriptive diagram for a sample with dimensions (3 × 40 × 80mm) is presented in

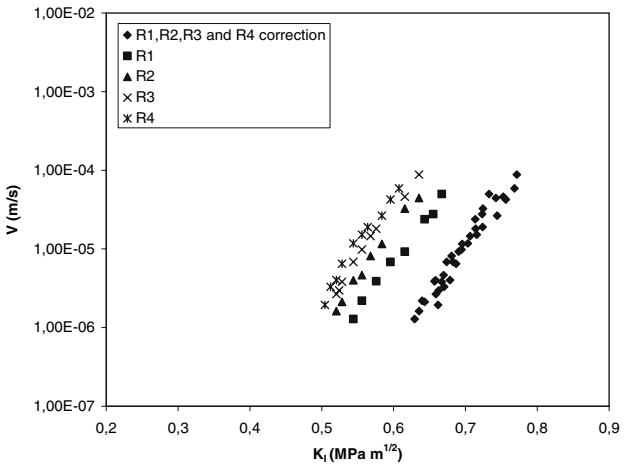

Fig. 11 Application of Chevalier's corrected equation on the preceding sample (3 × 40 × 70mm)

Fig. 12. The crack length difference Δa between the compressive and tensile sides corresponds to about five times the thickness ($\Delta a \approx 5t$) as observed by Evans [5]. Further observations are necessary to precisely study the effect of the surface crack variation.

Discussion

The experimental results showed that it is necessary to use sufficiently long samples (L/W ≥ 3) in order to have a large work domain where the stress intensity factor can be considered independent of the crack length. For such samples, Evans model can reliably be used for describing sub-critical crack growth on advanced crack lengths. As the sample length decreases (L/W < 3), the work domain is increasingly reduced. This leads to a clear dependency of the stress intensity factor on crack length that needs to be corrected.

The application of the corrected equation proposed by Chevalier (Eq. 13) showed that the exponent α depends on the sample geometry (L/W). The corrected V–K_I diagrams induce, however, an overestimation of the stress intensity factor related to the exponent value. Comparatively to admitted glass stress corrosion exponent n, these diagrams resulted in slight increased values.

At first sight, the use of the corrective factors derived in Ciccotti's finite element analysis on one example brings out better results on advanced crack lengths. This type of analysis could be closely adapted to the sample geometry and the loading configuration used. According to this analysis, the stress intensity dependency is related to the compliance non linear variation with crack length. Through the experimental compliance tests made on the different glass samples, this non linearity was not perceptible. The

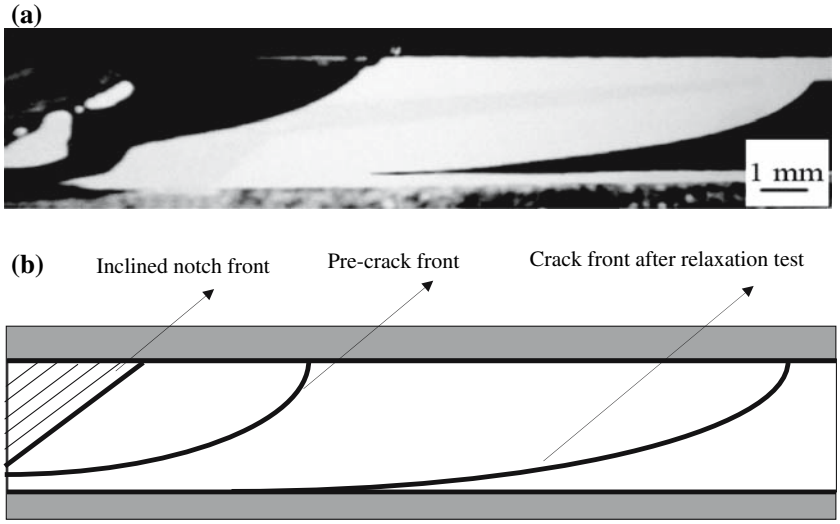

Fig. 12 Photograph of crack front profile on a sample with dimensions ($3 \times 40 \times 80$mm (**a**) and descriptive diagram of the photograph (**b**)

obtained linear variations on the different samples showed slopes closely comparable to Evans theoretical value and a coefficient D (ordinate at the origin) that varies with the sample length. The effect of this coefficient was not considered on the simulation proposed (Eq. 15).

It can be also noticed that, in all the preceding equations, it is assumed that the derivative of the sample compliance as a function of the crack surface A is equal to the derivative with regard to the crack length a, by supposing that the crack front profile remains constant. This assumption should merit an examination which has not been made in this work. If it is not valid, it leads to an additional term which must be taken into account in the equations and can explain the observed experimental results.

Conclusion

This experimental study evaluates the applicability of the double torsion technique in characterizing sub-critical crack growth based on Evans model and the corrected analyses proposed by Chevalier and Ciccotti using soda-lime glass samples of different lengths. The corrections were introduced to palliate the observed dependency of the stress intensity factor on crack length. The application of Evans model without correction is conditioned by the use of sufficiently long samples ($L/W \geq 3$) and advanced crack lengths. As the sample length reduces ($L/W < 3$), corrections are needed because the work domain where the stress intensity factor can be considered independent of the crack length becomes limited. Corrections applied to such cases revealed the necessity to rely on a finite element analysis closely adapted to the geometrical and loading configurations used.

References

1. Freiman SW, Mulville DR, Mast PW (1973) J Mater Sci 8:1527
2. Gonzalez AC, Pantano CG (1990) J Am Ceram Soc 73:2534
3. Janssen C, (1980) Fracture characteristics of double cantilever drilled compression Specimen, Report No R-8047. Corning Glass Works, Corning NH
4. Outwater JO, Gerry DJ (1966) On the Fracture Energy of Glass, NRL Interim Contract Report, Contract NONR 3219 (01), AD 640848, University of Vermont, Burlington, Vt, Aug
5. Evans AG, (1972) J Mater Sci 7:1137
6. Williams DP, Evans AG, (1973) J Testing Evaluation 11:264
7. Fuller ER Jr (1979) In: Freiman SW (ed) Astm Stp 678. American Society for Testing and Materials, p 3
8. Timoshenko SP (1951) In: Goodier JN (ed) Theory of elasticity. Mc Graw Hill, New York
9. Pollet JC, Burns SJ (1979) J Am Ceram Soc 62:62
10. Shetty DK, Virkar AV, Hardward MB, (1979) J Am Ceram Soc 62:307
11. Pletka BJ, Fuller ER Jr, Koepke BG (1979) In: Freiman SW (ed) Astm Stp 678. American Society for Testing and Materials, p 18
12. Evans AG, Wiederhorn SM (1974) Int J Fract 10:379
13. Trantina GC (1973) J Am Ceram Soc 60:338
14. Shetty DK, Virkar AV (1978) J Am Ceram Soc 61:93
15. Chevalier J, Saadaoui M, Olagnon C, Fantozzi G (1996) Ceram Int 22:171
16. Ciccotti M (2000) J Am Ceram Soc 83:2737
17. Ciccotti M, Gonzalo G, Mulargia F (2000) Int J Rock Mech Min Sci 37:1103
18. Ciccotti M, Negri N, Gonzalo G, Mulargia F (2001) Int J Rock Mech Min Sci 38:569
19. Wiederhorn SM (1967) J Am Ceram Soc 50:407
20. Wiederhorn SM, Boltz LH (1970) J Am Ceram Soc 53:543
21. Lawn BR (1993) In: The fracture of Brittle Solids, 2nd edn. Cambridge University Press
22. Sglavo VM, Green DJ (1999) J Mater Sci 34:579
23. Annis CG, Cargill JS (1978) In: Bradt RC, Hasselmann DPH, Lange FF (eds) Fracture Mechanics of ceramics, vol 4. Plenum Press, New York, p 737
24. Chevalier J (1996) Thèse de Doctorat, Etude de la propagation des fissures dans une zircone 3Y-TZP pour applications médicales, INSA